

Rotating shaft's non-linear response statistics under biaxial random excitation, by path integration

Oleg Gaidai^{1*)}, Michael Dimentberg²⁾, Arvid Naess³⁾

¹⁾ Jiangsu University of Science and Technology, Zhenjiang, China

²⁾ Worcester Polytechnic Institute, Worcester, USA

³⁾ Norwegian University of Science and Technology, Trondheim, Norway

1 Abstract

2

3 The response of rotating shaft to random excitations is of practical concern for various rotor type engine design appli-
4 cations, with high level of potential external forces of stochastic nature.

5 Authors have studied extreme value statistics of random vibrations of a Jeffcott type rotor, modeled as multidimen-
6 sional dynamic system with non-linear restoring forces, under biaxial white noise excitation. The latter type of dy-
7 namic system is of wide use in stability studies of rotating machinery – from automotive to rocket turbo engine design.
8 In particular, the design of liquid-propellant turbo pump rocket engines may be a potential application area of the
9 studied system, due to the biaxial nature of the mechanical excitation, caused by surrounding liquid turbulent pressure
10 field.

11 In this paper, the extreme statistics of the rotor's non-linear oscillations has been studied by applying an enhanced
12 implementation of the numerical path integration method, benchmarked by a known analytical solution. The obtained
13 response probability distributions can serve as input for a wide range of system reliability issues, for example in ex-
14 treme response study of turbo-pumps for liquid-propellant rocket engines. Predicting extreme transverse random vi-
15 brations of shafts in rotating machinery is of importance for applications with high environmental dynamic loads on
16 Jeffcott type rotor supports.

17 The major advantage of using path integration technique rather than direct Monte Carlo simulation is ability to estimate
18 the probability distribution tail with high accuracy. The latter is of critical importance for extreme value statistics and
19 first passage probability calculations.

20 The main contribution of this paper is a reliable and independent confirmation of the path integration technique as a
21 tool for assessing the dynamics of the kind of stochastic mechanical models considered in this paper. By the latter
22 authors mean application of a unique and nontrivial analytical solution, that yields exact dynamic system response
23 distribution, therefore it provides absolutely reliable reference to be compared to. The potential for providing a good
24 qualitative understanding of the behavior of such systems is therefore available.

25

26 **Keywords:** Jeffcott rotor; Path integration; Monte Carlo; FFT; non-linear restoring force; Fokker–Planck-

27 Kolmogorov equation.

28

29 1 Introduction

30

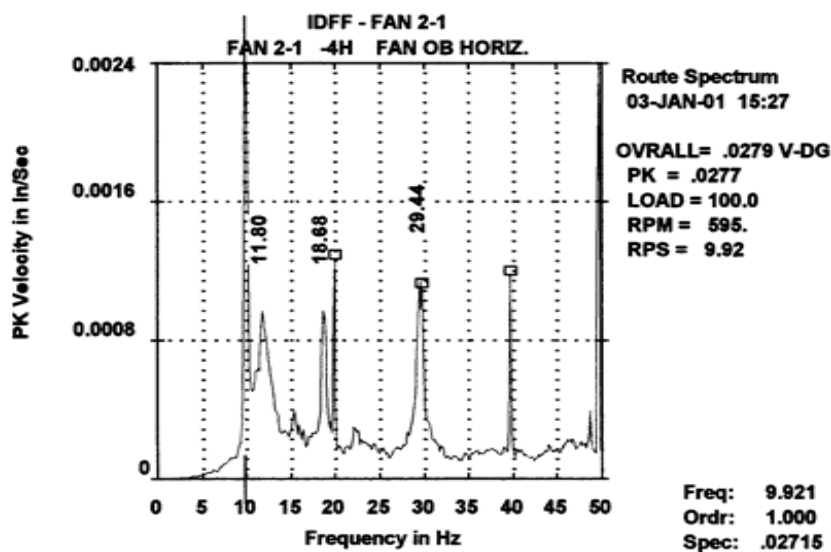
31 Jeffcott type rotating machinery can be found in a wide range of industrial areas: from automotive to airspace and
32 marine engines, see e.g. [3], [6]-[9]. The primary feature of Jeffcott type rotating machinery design is to deliver stability
33 under random and even extreme type of external excitations. The nature of stochastic exciting forces, acting from
34 outside and affecting rotor stability, is also quite different between say vehicle, airplane turbo fan, turbo-pump rocket
35 engine or submarine engine. From all above mentioned application areas, this paper applies mostly to turbo-pump
36 rocket engines, since biaxial random excitations have been studied.

37 The response of a rotating shaft to a biaxial random excitation is of practical concern for the design of liquid-propellant
38 turbo-pump rocket engines. Biaxial random excitation of the rocket engine shaft due to turbulence is an important
39 practical concern, especially for the purpose of improved stability; see [3], [6], [15]. The assumption of zero correlation
40 between two transverse components of biaxial excitation is always satisfied in the important case of excitations gener-
41 ated by a turbulent pressure field, which is delta-correlated in circumferential direction [6].

42 The nature of hydrodynamic turbulent pressure field is quite complex, for recent studies on VIV (vortex induced
43 vibrations) see e.g. [23], [24], where for the first time, the method developed in [23] provided the possibility to get
44 accurate distributions of hydrodynamics coefficients along a flexible shaft under turbulent pressure field conditions,
45 and became indispensable reference for that field.

46 Design of a turbo-pump for a liquid-propellant rocket engine may be quoted as an example whereby operation of the
47 shaft close to its instability threshold is of concern because of increased sensitivity of the whole system of shaft-
48 machine-vehicle to such loads [15]. On the other hand, small random vibration components may sometimes be ob-
49 served in turbulence affected rotating machinery (turbines, fans, etc.), [6], [15]. Figure 1 from [22] presents the spectral
50 density of the vibration signal from the bearing of a large fan with a dominant peak at the rotational frequency 9.92 Hz
51 and neighboring peak at the shaft's resonance at 11.80 Hz.

52



53

54 **Figure 1** Spectral density of the vibration signal from the bearing of a large fan with dominant peak at the rotational

55 frequency 9.92 Hz and neighboring peak at the shaft's resonance at 11.80 Hz.

56

57 Since the fan rotational response itself is of narrow band stable nature, the resonant multi-peaked excitation is due to
58 a wide band white noise-like ambient turbulence. As long as any modal generalized force is derived from the turbulence
59 field by proper spatial integration, the Gaussian model seems reasonable. The latter point is in view of the basic theo-
60 rems of asymptotic Gaussianity for linear systems' response with a high excitation/system bandwidth ratio.

61 Because Jeffcott type systems present significant engineering interest, this paper aims at contributing to the study of
62 Jeffcott-type mechanical systems, namely studying statistics of the system response, specifically the transverse/radial
63 shaft displacement. Radial motions are of importance for system stability and design issues. The restoring force in the
64 shaft of the Jeffcott rotor is modelled as elastic non-linear, which corresponds to a realistic engineering case. Both
65 internal (rotating) and external damping have been included in the studied rotor mechanical model.

66 Statistics of the rotor's non-linear oscillations is studied by applying the path integration (PI) method, which relies on
67 the Markov property of the coupled dynamical system. By Markov property one means that the probabilistic behaviour
68 of the future response increment depends only on the present response value and discards its past behaviour, see e.g.
69 [1], [4]. The Jeffcott rotor response statistics was obtained by solving the Fokker–Planck–Kolmogorov equation [4] for
70 the corresponding 4D dynamic system. In order to study probability distribution of the system response, an efficient
71 modification of the PI algorithm is introduced, based on the fast Fourier transform (FFT), to calculate the response
72 statistics of a dynamic system with additive noise. The latter allows a significant reduction of the computational time,
73 compared to the classical PI. The excitation force is modelled as Gaussian white noise; however, any noise process
74 with stationary, independent increments with known distribution, can be implemented with analogous PI technique. It
75 should be noted, however, that the path integration (PI) methodology presented in this paper, equally applies to a
76 uniaxial excitation force. The latter makes the PI technique relevant for a wide range of Jeffcott type rotating shaft
77 applications: not only in fluid machinery, but also in transport, [5], [12], [21].

78

79 The numerical path integration technique (see e.g. [1], [4], [21]) is well known as an efficient approximation for solving
80 the Fokker–Planck–Kolmogorov equation, and giving accurate estimates of stationary response PDF (probability den-
81 sity functions) for dynamic systems. The base of PI method is the Markov property of dynamic system (the latter is
82 expressed as an equivalent system of first order differential equations). Then the evolution of the response PDF is
83 estimated via a step-by-step solution scheme, based on reasonably short time steps. In more detail, the response PDF
84 at a current time instant can be estimated, if the response PDF at an earlier discrete time instant, and the conditional
85 PDF (which in this paper is of Gaussian form) are already known.

86

87 The PI solution suggested in this paper has been accelerated by using a pre-estimated joint probability density function
88 (PDF) as an initial input. Pre-estimation of the stationary PDF has been done by Monte Carlo (MC) simulation.

89 The main objective of studying statistics of the non-linear case by applying a 4D path integration (PI) method, was to
90 obtain a sufficiently high resolution of the stationary response PDF tail (specifically at quite low probability levels). A
91 major advantage of PI method compared to e.g. direct Monte Carlo Simulation (MCS) has been demonstrated in details
92 in this paper. The latter suggests PI methodology as a practical engineering/design tool for performing reliability anal-
93 ysis of Jeffcott type rotating shafts (and other related mechanical systems).

94 Finally, in order to validate the accuracy of the proposed numerical PI scheme, a comparison has been done with an
95 available exact analytical solution of the joint response probability density function (PDF), see [12].

96

97 2 Dynamic analysis

98

99 Numerous studies have been done to study non-linear effects in rotor dynamics [8], [9], [16]-[20]. This paper considers
100 a Jeffcott rotor with non-linear restoring force. Then the linearized axisymmetric combined shaft/support lateral stiff-
101 ness is denoted K ; the shaft angular velocity is denoted ν .

102 The shaft carries a disk of mass m located at its mid-span and has both external (“non-rotating”) damping and internal
103 (“rotating”) damping. The shaft external and internal damping coefficients in this paper are denoted as c_n and c_r re-
104 spectively.

105 The shaft’s Z -axis is modelled to be horizontal and external exciting forces are applied along both transverse directions
106 X and Y . Then, by neglecting gravity forces for sufficiently high rotation speeds and adding the transverse forces, the
107 following equations of the disk lateral motion [5], [12] can be obtained

108

$$\ddot{X} + 2\kappa\dot{X} + f_X(X, Y) + 2\beta\nu Y = \gamma\dot{W}_1(t); \quad \ddot{Y} + 2\kappa\dot{Y} + f_Y(X, Y) - 2\beta\nu X = \gamma\dot{W}_2(t) \quad (1)$$

109

110 with $\kappa = \alpha + \beta$, $\alpha = c_n/2m$, $\beta = c_r/2m$. $\dot{W}_k(t)$ being stationary, independent zero-mean Gaussian white noises, be-
111 ing formal derivatives of Wiener processes $W_k(t)$ with normally distributed increments with $E[dW_k(t)] = 0$ and
112 $E[dW_k(t)dW_k(s)] = dt$ for $t = s$, and $= 0$ for $t \neq s$; $k = 1, 2$. Noise intensities are assumed to be the same for both
113 transverse directions, and are denoted by γ . Note that the dynamic system (1) is an axisymmetric (biaxial) Jeffcott
114 system, see [12], where the analytical solution to the Fokker–Planck–Kolmogorov equation has been obtained.

115

116 The non-linear elastic restoring force components along X and Y axes are denoted $f_X(X, Y)$ and $f_Y(X, Y)$, respectively.
117 The non-linear version of the restoring forces studied in this paper, is assumed to be given as in [9]:

118

$$f_X(X, Y) = \Omega^2 X \cdot [1 + f(r)]; \quad f_Y(X, Y) = \Omega^2 Y \cdot [1 + f(r)]; \quad f(r) = \left[1 - \frac{1}{\sqrt{1 + R^2}}\right] \tilde{\varepsilon} \quad (2)$$

119

120 with $\Omega^2 = K/m$, and $r(X, Y) = \sqrt{X^2 + Y^2}$, $\varepsilon = T/EA \ll 1$, $\tilde{\varepsilon} = \varepsilon^{-1} - 1 > 0$, with T being the reference (constant)
121 tension in the shaft, corresponding to its horizontal position, i.e. $T = EA\varepsilon$, thus ε is actually the shaft inverse stiffness
122 parameter. It is worth noting that in this paper the shaft is assumed to be perfectly balanced. As mentioned above, X
123 and Y are being non-dimensionalized displacements, representing actual radial shaft transverse displacements u and v
124 by scaling, $X = u/L$, $Y = v/L$ with L being the half distance between two shaft supports [9].

125 Since the main focus of this paper is extreme response statistics, linearization of the restoring force was not appropriate.
126 Therefore, an efficient PI technique has been applied, enabling high accuracy estimation of the PDF tails, without
127 simplifying system nonlinearities.

128

129 The dynamic system represented by Eq. (1) can be equivalently re-written as a four dimensional (4D) first order dif-
130 ferential system by introducing the 4D state space variable $\mathbf{x} = (x_1, y_1, x_2, y_2)$, where $x_1 = X$, $y_1 = Y$, $x_2 = \dot{X}$, $y_2 =$
131 \dot{Y} ,

132

$$\begin{aligned}
dx_1 &= x_2 dt \\
dy_1 &= y_2 dt \\
dx_2 &= (-2\kappa x_2 - f_Y(x_1, y_1) + 2\beta v y_1) dt + \gamma dW_1 \\
dy_2 &= (-2\kappa y_2 - f_X(x_1, y_1) - 2\beta v x_1) dt + \gamma dW_2
\end{aligned} \tag{3}$$

133

134

135 3 Path integration method

136

137 The dynamic system given by equation (3) belongs to a class of Markov diffusion processes [10]. Thus, system (3) can be
138 studied using Itô stochastic differential equation (SDE)

139

$$dx = \boldsymbol{\mu}(\mathbf{x}, t)dt + \boldsymbol{\sigma}(t)d\mathbf{W}(t) \tag{4}$$

140

141 where $\mathbf{x}(t) = (x_1, \dots, x_n)^T$ is an n -dimensional vector, as is $\boldsymbol{\mu}(\mathbf{x}, t)$; $\boldsymbol{\sigma}(t)$ is an $n \times n$ matrix, and $\mathbf{W}(t)$ being an n -
142 dimensional standard Wiener vector process, with dimension $n = 4$. Then the state space vector $\mathbf{x}(t)$ being a Markov
143 process and its transition probability density (TPD) $p(\mathbf{x}, t | \mathbf{x}', t')$ will satisfy the following well known Fokker–Planck–
144 Kolmogorov (FPK) equation [16], [17].

145

$$\begin{aligned}
\frac{\partial}{\partial t} p(\mathbf{x}, t | \mathbf{x}', t') &= - \sum_{k=1}^n \frac{\partial}{\partial x_k} (\mu_k(\mathbf{x}, t) p(\mathbf{x}, t | \mathbf{x}', t')) \\
&+ \frac{1}{2} \sum_{k,l=1}^n \frac{\partial}{\partial x_k} \left(\sigma_{kl}(\mathbf{x}, t) \sum_{m=1}^n \left[\frac{\partial}{\partial x_m} \sigma_{ml}(\mathbf{x}, t) p(\mathbf{x}, t | \mathbf{x}', t') \right] \right)
\end{aligned} \tag{5}$$

146

147 PI method estimates the probabilistic evolution of $\mathbf{x}(t)$ by means of taking advantage of the system Markov property.
148 The numerical PI is an approximate approach and the PDF of the process $\mathbf{x}(t)$ can be estimated by referring to the
149 following equation

150

$$p(\mathbf{x}, t) = \int_{\mathbb{R}^n} p(\mathbf{x}, t | \mathbf{x}', t') p(\mathbf{x}', t') d\mathbf{x}' \tag{6}$$

151

152 with $d\mathbf{x}' = \prod_{k=1}^n dx_k$. The PDF $p(\mathbf{x}, t)$ at time t can be calculated from Eq. (7) based on knowledge of the TPD
153 $p(\mathbf{x}, t | \mathbf{x}', t')$ and the values of the previous PDF $p(\mathbf{x}', t')$ at time t' . For a numerical solution of the stochastic differ-
154 ential equation (4), a time-discretized approximation has been employed. In [4] the fourth-order Runge–Kutta–
155 Maruyama (RKM) discretization approximation has been presented

156

$$\mathbf{x}(t) = \mathbf{x}(t') + \mathbf{h}(\mathbf{x}(t'), \Delta t') + \boldsymbol{\sigma}(t') \Delta \mathbf{W}(t') \tag{7}$$

157

158 where the vector $\mathbf{h}(\mathbf{x}(t'), \Delta t')$ being an explicit fourth-order Runge–Kutta (RK4) approximation. Since $\mathbf{W}(t)$ is a
159 Wiener type process, the noise increment $\Delta \mathbf{W}(t') = \mathbf{W}(t) - \mathbf{W}(t')$ is a Gaussian variable for every time instant t' and
160 t . The time sequence $\mathbf{x}(k\Delta t')$, $k = 0, \dots, \infty$, is a Markov chain approximating the time-continuous Markov process
161 solution of the stochastic differential equation (4), while the time increment $\Delta t' = t - t'$ being small enough, and the

162 spatial mesh for the \mathbf{x} -variable being fine enough.

163

164 Note that, as mentioned in [11], the interpolation error at each time step will be about the same order of magnitude
165 and will be independent of the time step magnitude, thus the final solution may give a larger final error for shorter time
166 steps, because more iterations are required to reach stationary response state. In practical applications, for higher di-
167 mensional systems, a very fine mesh cannot be numerically afforded, thus the time step can not be chosen arbitrarily
168 small.

169 Since the expression for the TPD is known (two independent one-dimensional Gaussian distributions in this paper),
170 the time evolution of the PDF of $\mathbf{x}(t)$ can be estimated by the following iterative equation

171

$$p(\mathbf{x}, t) = \int_{\mathbb{R}^n} \dots \int_{\mathbb{R}^n} \prod_{k=1}^N p(\mathbf{x}^{(k)}, t_k | \mathbf{x}^{(k-1)}, t_{k-1}) p(\mathbf{x}^{(0)}, t_0) d\mathbf{x}^{(0)} \dots d\mathbf{x}^{(N-1)} \quad (8)$$

172

173 with $p(\mathbf{x}^{(0)}, t_0)$ being an initial PDF, and $\mathbf{x} = \mathbf{x}^{(N)}$; $t = t_N = t_0 + N\Delta t$. In this paper authors has proposed to esti-
174 mate initial PDF from prior Monte Carlo (MC) simulation, in order to accelerate solution convergence, specifically to
175 reduce a number of necessary time steps N before the converged solution can be obtained.

176

177 **4 Efficient numerical implementation**

178

179 The iterative solution technique of the PI approach is presented by Eq. (8). For numerical implementation of the PI
180 method, a proper computational domain and the corresponding computational grid (carrier domain) have to be esti-
181 mated at first. For more detailed description of the numerical iterative algorithm see [19], [20]. Larger higher dimen-
182 sional grids naturally lead to a larger size of variables and to a longer computational time. In [18] it is suggested to use
183 GPU for a computational speed up, as compared to CPU based implementation. The problem with the latter suggestion
184 is that the GPU memory capacity (VRAM) is much less than the CPU memory capacity (RAM).

185

186 In this paper, the initial PDF $p(\mathbf{x}^{(0)}, t_0)$ and its carrier domain have been estimated from the prior extensive MC
187 simulation of the dynamical system of type (3) over a sufficiently long time period T . The latter choice of the pre-
188 estimated initial PDF by MCS is proven to enable faster convergence of the iterative algorithm (8) within a reasonably
189 shorter number of time steps N . Note, that the initially pre-estimated joint PDF by MCS is not accurate in the PDF tail
190 area (namely for low probability levels); thus it is a task of the subsequent PI calculation to develop a converged
191 solution with accurate PDF tails.

192

193 Numerically, the joint PDF at any time t is being approximated using interpolated parabolic B-spline surface. Then,
194 the RK4 approximation scheme is applied to estimate the deterministic trajectories backward for each \mathbf{x} -grid point.
195 Thus, each \mathbf{x} -grid point at each time t is mapped backwards with the corresponding starting point at the previous time
196 t_0 and the PDF values at the backward-mapped points, i.e., the starting points, can be given by using the B-spline
197 surface. Finally, the PDF at time t can be calculated by substituting the TPD $p(\mathbf{x}, t | \mathbf{x}', t')$ (normally distributed in the
198 case of this paper) into Eq. (6). Furthermore, the capability of the PI method in producing accurate and reliable solutions
199 for stochastic dynamic systems was demonstrated by numerous studies, see e.g. [1], [4].

200

201 The mean up-crossing rate is an important parameter for estimation of the large and extreme response statistics as well
 202 as for evaluation of the associated reliability of dynamic structures, subjected to random external forces [2]. The radial
 203 displacement r of the disk when approaching the casing circular wall of the turbo fan can be regarded as a high re-
 204 sponse level. Alternatively, one can study von Mises stresses in the shaft as a response of interest. For the latter purpose,
 205 the same methodology as described here will apply. The estimation of the mean up-crossing rate of the radial response
 206 R of the level ξ is usually based on the Rice equation

$$v^+(\xi, t) = \int_0^\infty \dot{r} p_{RR}(\xi, \dot{r}) d\dot{r} \quad (9)$$

208
 209 The 2D joint PDF p_{RR} can be extracted from the 4D PI joint PDF $p(\mathbf{x}, t)$ in (8). In case when the assumption of
 210 statistically independent up-crossing is valid for a certain level in this region, the corresponding crossing events are
 211 Poisson distributed. Under the latter assumption, the reliability evaluation is usually phrased in terms of the probability
 212 that the disk vertical displacement X exceeds the specific threshold at least once during a time interval of length T .
 213 Thus, the exceedance probability for duration of exposure time T can be approximated by the following widely used
 214 approach

$$P_\xi(T) = 1 - \exp\left(-\int_0^T v^+(\xi, t) dt\right) \approx 1 - \exp(-v^+(\xi)T) \approx v^+(\xi)T \ll 1 \quad (10)$$

215
 216 where $v^+(\xi)$ represents the mean up-crossing rate of the level ξ (radial transverse displacement r in this paper) at a
 217 suitable reference point in time, which can be estimated directly by the 4D PI method and the Rice Eq. (9).

218

219

220 5 Numerical results

221

222 In this section the non-linear system (1), (2) statistical results are compared with corresponding analytical solution that
 223 is available. Also, the stability margin is well known for the linear case. The linearized (namely linearized restoring
 224 force) system (1), (2) possesses the following dynamic stability condition $v < v_*$, provided in [3], [7]

225

$$v < v_* = \frac{\kappa\Omega}{\beta} = \Omega \left(1 + \frac{c_n}{c_r}\right) \quad (11)$$

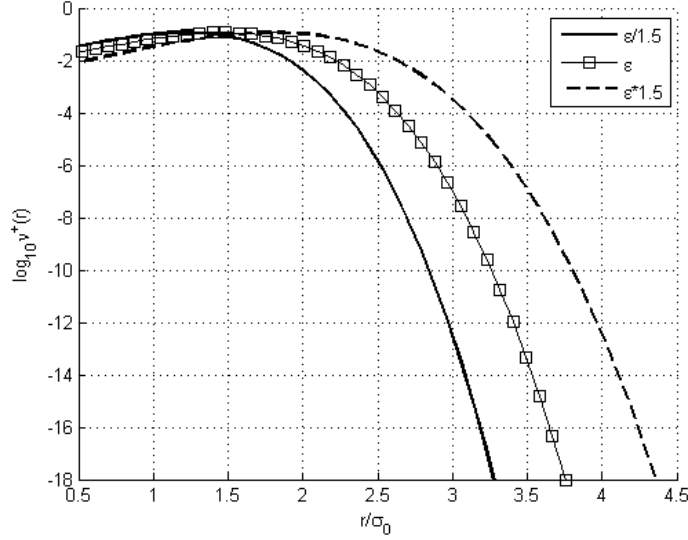
226

227 For the case $\Omega = 1$, $\alpha = \beta = 0.02$, $\gamma = 0.02$, Eq. (11) gives a linearized stability margin $v^*/\Omega = 2$. In this paper a
 228 computational mesh for the 4D variable \mathbf{x} in the equivalent system (3) has been chosen with following grid resolution
 229 $128 \times 128 \times 128 \times 128$. Regarding the small stiffness parameter $\varepsilon = T/EA$ in Eq. (2), for the non-linear restoring force it
 230 is chosen to be equal 0.1.

231 In brief the effect of varying the force stiffness parameter $\varepsilon = T/EA$ on the transverse radial displacement mean up-
 232 crossing rate for the non-linear dynamic system (1), (2). Keeping the shaft tension T constant, while increasing the
 233 shaft stiffness EA , will decrease the shaft stiffness parameter ε , and yield a decrease in the transverse radial amplitude.
 234 The latter phenomenon is clearly seen from Figure 2.

235

236



237

238

239 **Figure 2** Effect of the shaft stiffness parameter ε on the radial displacement up-crossing rate, for the non-linear dy-
 240 namic system (1), (2).

241

242 In the case of purely additive white noise, independently acting in two different dimensions, the PI algorithm can be
 243 implemented by performing the PI integration by means of the Fourier transformation, see e.g. [16]. The FFT (fast
 244 Fourier transform) numerical implementation is based on the path integral (8), Section 3, being represented as two pure
 245 consequent convolutions (for the case of additive white noise entering two different system dimensions). This requires
 246 the full Jacobian method that is used in this paper. Since the Fourier transform of the convolution is a simple product,
 247 and computing a product is numerically much more efficient than a convolution integral, it is CPU time-saving to use
 248 the FFT algorithm for the additive noise PI. Since the FFT method is not exact, its numerical accuracy can be further
 249 enhanced by choosing a sufficiently high grid resolution and mesh span.

250

251 5.1 Analytical solution

252

253 In this subsection the following parameters are chosen for the system (1), (2): $\Omega = 1$, $\alpha = \beta = 0.02$, $\nu = 2.2$, and the
 254 linear dynamic stability condition (11) $\nu < \nu_*$ does not hold. In [12] an analytical solution $p(x_1, y_1, x_2, y_2)$ was estab-
 255 lished that satisfies the Fokker-Planck-Kolmogorov equation

256

$$\begin{aligned}
 x_2 \frac{\partial p}{\partial x_1} + \frac{\partial}{\partial x_2} \{ \Omega^2 [1 + f(r)] x_1 p + 2\kappa x_2 p + 2\beta \nu y_1 p \} - y_2 \frac{\partial p}{\partial y_1} \\
 + \frac{\partial}{\partial y_2} \{ \Omega^2 [1 + f(r)] y_1 p + 2\kappa y_2 p - 2\beta \nu x_1 p \} + \frac{\gamma^2}{2} \left(\frac{\partial^2 p}{\partial x_2^2} + \frac{\partial^2 p}{\partial y_2^2} \right) = 0
 \end{aligned} \tag{12}$$

257

258 with $r = \sqrt{x_1^2 + y_1^2}$. Direct substitution shows that the partial differential equation (12) has the following exact ana-
 259 lytical solution

260

$$p(x_1, y_1, x_2, y_2) = C \cdot \exp \left[-\frac{4\kappa}{\gamma^2} H + \frac{4\beta\nu}{\gamma^2} (x_1 y_2 - x_2 y_1) \right], \quad H = \frac{\Omega^2}{2} (r^2 + F(r)) + \frac{1}{2} (x_2^2 + y_2^2), \quad \text{where } \frac{dF}{dz} = f, \text{ and } z = r^2 \quad (13)$$

261

262 with C being a normalization constant which is obtained by requiring that the integral of the expression (13) over \mathbb{R}^4 is
 263 equal to 1.0; function f is defined in (2). The solution of the form (13) is well known for the case of the symmetric
 264 apparent nonlinear stiffness matrix in the original equation of motion (1), that is for $\nu = 0$, see [12], [13], [14].

265

266 5.2 Comparison between path integration results and the analytical solution

267

268 In this subsection the following parameters are chosen in system (1)-(2): $\Omega = 1, \alpha = \beta = 0.02, \nu = 2.2$, and the linear
 269 dynamic stability condition (11), $\nu < \nu_*$, is not satisfied. Since the biaxial excitation force, studied in this paper, has
 270 radial symmetry (as opposed to the uniaxial excitation force), it is expedient to consider the transverse radial displace-
 271 ment $r = \sqrt{X^2 + Y^2}$. In particular, the mean up-crossing rate will be studied. For this purpose, it is convenient to
 272 change coordinates from (x_1, y_1, x_2, y_2) to $(r, \dot{r}, \theta, \dot{\theta})$ with (r, θ) being polar coordinates for $(x_1, y_1) \equiv (X, Y)$. Then,
 273 a coordinate transformation leads to the following PDF relation $p(r, \dot{r}, \theta, \dot{\theta}) = p(x_1, y_1, x_2, y_2) \cdot r^2$. This allows the
 274 calculation of the mean up-crossing rate $\nu^+(r)$ of the radial displacement by invoking Rice's formula (9).

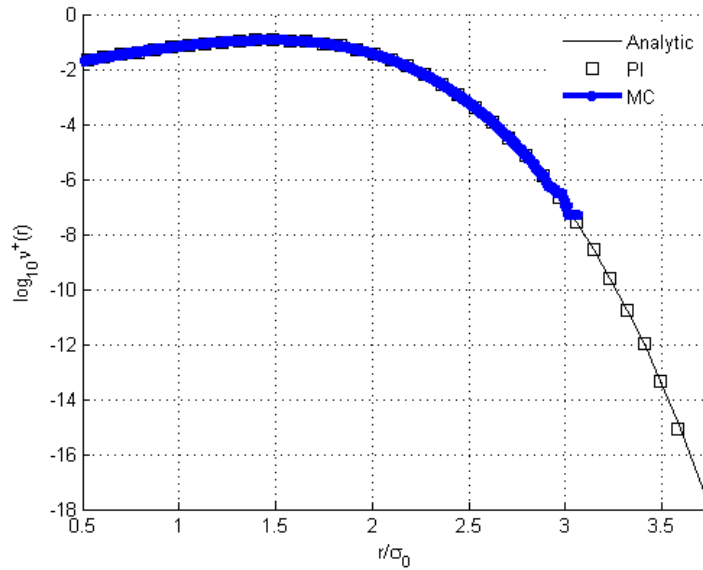
275

276 Figure 3 presents the mean up-crossing rate of the transverse radial response for the non-linear dynamic system (1), (2)
 277 obtained by the three methods available here. It is seen from Figure 3 that PI offers highly accurate estimates of the
 278 radial response at low probability levels, compared to extensive MC simulation. Note that CPU time spent in order to
 279 obtain both MC and PI simulation results, presented in Figure 3, is about the same order, while PI gives upto 8 orders
 280 of magnitude deeper crossing rate tail resolution. The latter effectively means that PI provides much more accurate
 281 probability tail distribution, than MC, provided same CPU time spent. Thus the PI may offer a significant advantage,
 282 with respect to the straightforward MC, since in many engineering design applications multiple numerical simulations,
 283 corresponding to different dynamic system numerical parameter setups, often have to be run.

284 Regarding error analysis for numerical methods such as MC and PI, since Figure 3 presents good match with analytical
 285 (exact) probability tail, it is clear that numerics has been performed accurately. Both PI and MC could have been
 286 compared in terms of the relative error for the predicted response level at a given low probability of interest, since an
 287 exact analytical solution is available. However since MC simulation provides much more "shallow" probability distri-
 288 bution tail, for the same CPU time spent as for PI, comparison between only PI and exact solution was done at the
 289 probability level 10^{-15} ; the relative error of PI method for the latter response level was less than 5%.

290 The reference value σ_0 is the corresponding standard deviation of r -response for the case of linear restoring force.
 291 Reaching probability levels of order 10^{-15} is simply unaffordable with direct MC simulation, given the requirement
 292 of a small time-step and limited CPU time. PI however manages the latter task within a relatively small number of time
 293 steps (due to initial PDF pre-calculation by MC) and at low computational PI cost (due to the FFT based implementa-
 294 tion). Therefore, PI becomes an efficient tool for a study of the reliability or extreme value statistics of the Jeffcott
 295 systems of type (1).

296



297

298 **Figure 3** Mean up-crossing rates for non-linear system, transverse radial displacement: MC (*) versus PI (□) versus
 299 analytical solution (—).

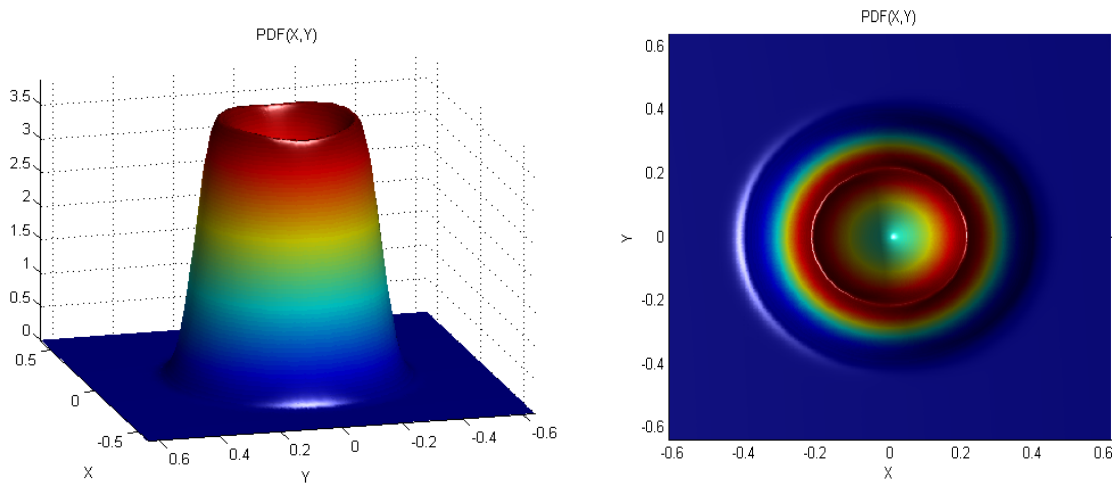
300

301 Figure 4 presents the stationary joint 2D PDF(X, Y) of the non-linear dynamic system (1), (2), extracted from the 4D
 302 PDF solution $p(\mathbf{x}, t)$ of the PI equation (8), where $\mathbf{x} = (x_1, y_1, x_2, y_2)$, see Section 5.1. Figure 5 presents the contour
 303 lines of the joint PDF(X, Y), corresponding to Figure 4. It is seen from Figure 5 that the PDF contour lines are axisym-
 304 metric, as expected due to axial symmetry of the dynamic system (1), (2) itself.

305

306

307



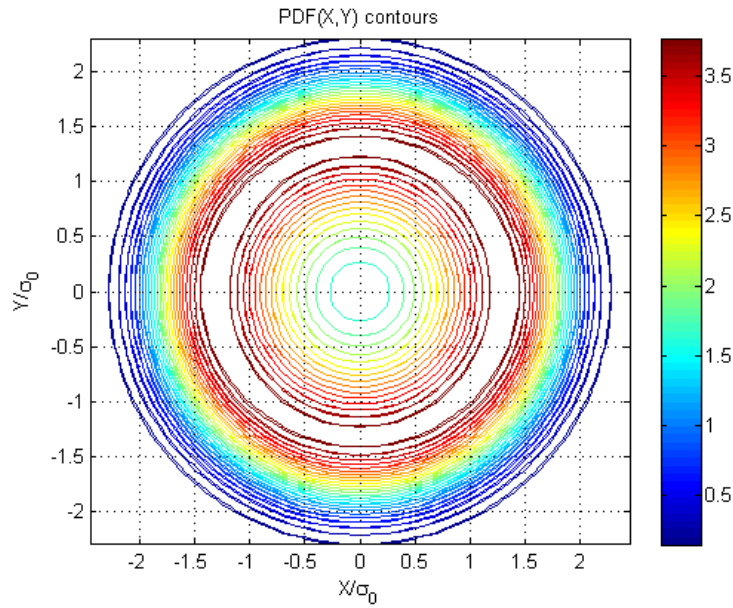
308

309 **Figure 4** Stationary joint PDF(X, Y) for non-linear dynamic system (1), (2); top view on the right.

310

311

312



313
 314 **Figure 5** Contour lines for the stationary joint PDF(X, Y) presented in Figure 4 for the non-linear dynamic system
 315 (1), (2).
 316

317 Note that for the parameter choice made in this subsection, the linearized system is unstable. As one can see from the
 318 presented figures, the non-linear system is still stable due to restoring force non-linearity. This is an important practical
 319 observation, since in reality restoring forces are indeed non-linear. The existence of a stationary response PDF implies
 320 stability of the self-excited response. The instability threshold may be estimated easily by the switch from unimodal to
 321 bimodal PDF.
 322

323 6 Conclusions

324
 325 In this work, the Jeffcott type rotor with non-linear restoring force subject to biaxial white noise excitation has been
 326 studied. Statistics of the rotor shaft transverse response was studied. The theory of Markov processes was used in
 327 modelling the rotor dynamics in a state space formulation, and the 4D PI approach based on the Markov property of
 328 the dynamic system was found to be in a good agreement with available analytical solution, proving high accuracy of
 329 the suggested numerical technique. Comparison with analytical results demonstrated efficiency, robustness and relia-
 330 bility of the 4D PI method.
 331

332 In this paper, the PI approach has been reinforced by using MC and FFT, which significantly reduces both computa-
 333 tional effort and the number of iterations needed for convergence to a stationary solution. In overall, the proposed
 334 technique is proven to be highly accurate and more efficient than direct MC estimation of extreme response with low
 335 probability levels.

336 The accuracy of PI is demonstrated by estimating the mean up-crossing rate at low probability levels. For ergodic
 337 random processes the mean up-crossing rate is known to be a key factor for studying reliability and extreme value
 338 statistics.
 339

340 Naturally, often question about advantage of PI over direct MC arises. With regard to extreme value statistics, first
 341 passage probability, defining design values, etc. for rotating machinery – it is clear that direct MC is computationally

342 expensive when very low probabilities are targeted, moreover when numerous system parameters are to be optimized
343 at the mechanical system design stage.

344 Another point of skepticism about PI is that it is seldom used for systems with number of degrees of freedom higher
345 than four (4D). Here it is worth noting that recent advances in GPUs (Graphic Processing Unit) do enable 6D PI
346 solutions, and obviously this is not a final limit for PI.

347
348 As shown in this paper, the non-linear system is still stable for the parameter set where the linearized system is unstable
349 (here authors refer to the dynamic instability condition from [7]). In this paper the restoring force non-linearity (and
350 therefore dynamic system non-linearity as a whole) was responsible for the system dynamic stability. This observation
351 is of practical importance, since in practice restoring forces are non-linear. Also, the structure of the response joint
352 PDF is observed to be strongly non-Gaussian, when exceeding the stability margin. Finally, convergence of the PI
353 solution to the stationary PDF implies stability of the (hardening) nonlinear system's response in case of the instability
354 of the linearized system.

355

356 **Conflict of interests statement**

357 The authors declare that they have no conflict of interest.

358 **References**

359 [1] W. Chai, A. Naess, B. J. Leira, Stochastic dynamic analysis and reliability of a vessel rolling in random beam
360 seas, *Journal Ship Research*, 2015, Vol. 59(2), pp. 113-131.

361 [2] A. Naess, T. Moan, *Stochastic Dynamics of Marine Structures*, 2012, New York, Cambridge University Press.

362 [3] M. F. Dimentberg, A. Naess, L. Sperling, Response of a rotating shaft to uniaxial random excitation, *J. Appl.*
363 *Mech.*, 2012, Vol. 79(4).

364 [4] A. Naess, V. Moe, Efficient path integration methods for nonlinear dynamic systems, *Probabilistic Engineering*
365 *Mechanics*, 2000, Vol. 15, pp. 221–231.

366 [5] M. Gobbi, F. Levi, G. Mastinu, Multi-objective stochastic optimization of the suspension system of road vehicles,
367 *Journal of Sound and Vibration*, 2006, Vol. 298, pp. 1055–1072.

368 [6] M. F. Dimentberg, B. Ryzhik, L. Sperling, Random vibrations of a damped rotating shaft, *J. Sound Vibration.*,
369 2005, Vol. 279(1-2), pp. 275-284.

370 [7] C. W. Lee, *Vibration analysis of rotors*, 1993, Kluwer, Dordrecht.

371 [8] Y. Ishida, Non-linear vibrations and chaos in rotor dynamics, *JSME International Journal, Series C*, 1994, Vol.
372 37(2), pp. 237-245.

373 [9] G. Adiletta, A. R. Guido, C. Rossi, Non-periodic motions of a Jeffcott rotor with non-linear elastic restoring

- 374 forces, *Nonlinear Dynamics*, 1996, Vol. 11, pp. 37-59.
- 375 [10] A. H. Jazwinski, *Stochastic processes and filtering theory*, 2007, New York, Dover Publications.
- 376 [11] J. M. Johnsen, *Response statistics of nonlinear dynamic systems*, PhD thesis, NTH, Norway, August 1992.
- 377 [12] M. F. Dimentberg, Non-linear random vibrations of rotating shaft, *ZAMM, Journal of Applied Mathematics and*
378 *Mechanics*, 2005, Vol. 85(3), pp. 211-212.
- 379 [13] M. F. Dimentberg, *Statistical dynamics of nonlinear and time-varying systems*, 1989, Research studies press,
380 Taunton.
- 381 [14] Y. K. Lin, C. Cai, *Probabilistic structural dynamics*, 1995, McGraw-Hill, New York.
- 382 [15] H. Motoi, A. Kitamura, N. Sakazume, M. Uchimi, M. Uchida, K. Saiki, O. Nozaki, T. Iwastubo, Sub-synchronous
383 whirl in the Le-7a rocket engine fuel turbo-pump, 2003, *Proceedings of the 2nd symposium on stability control of*
384 *rotating machinery (ISCORMA-2)*, Gdansk, Poland, pp. 160-169.
- 385 [16] E. Mo, A. Naess, Efficient path integration by FFT. In *Proceedings 10th International Conference on Applications*
386 *of Statistics and Probability in Civil Engineering (ICASP10)*, 2007, Tokyo, Japan.
- 387 [17] I. Kougiumtzoglou P. Spanos, An analytical Wiener path integral technique for non-stationary response deter-
388 mination of nonlinear oscillators, *Probabilistic Engineering Mechanics*, 28, pp. 125-131, 2012.
- 389 [18] P. Alevras, D. Yurchenko, GPU computing for accelerating the numerical Path Integration approach, *Computers*
390 *& Structures*, 171, pp. 46-53, 2016.
- 391 [19] D. Yurtchenko, E. Mo, A. Naess, Response probability density functions of strongly non-linear systems by the
392 path integration method, *Int. J. Non-Linear Mech.* 41, 693–705, 2006.
- 393 [20] D. Yurchenko, A. Naess, P. Alevras, Pendulum's rotational motion governed by a stochastic Mathieu equation,
394 *Probab. Eng. Mech.* 31, 12–18, 2013.
- 395 [21] O. Gaidai, A. Naess, M. F. Dimentberg, Response statistics of rotating shaft with non-linear elastic restoring
396 forces by path integration, *Journal Sound and Vibration*, Vol. 400, pp.113-121, 2017.
- 397 [22] J. Hall, Private communication, 2003.
- 398 [23] L. Song, S. Fu, J. Cao, L. Ma, J. Wu, An investigation into the hydrodynamics of a flexible riser undergoing
399 vortex-induced vibration, *Journal of Fluid and Structures*, 63, pp. 325-350, 2016.
- 400 [24] W. Wei, S. Fu, T. Moan, et al., A discrete-modules-based frequency domain hydroelasticity method for floating
401 structures in inhomogeneous sea conditions, *Journal of Fluids and Structures*, 74, pp. 321-339, 2017 .